IRIS AperTO

UNIVERSITÀ DEGLI STUDI DI TORINO

AperTO - Archivio Istituzionale Open Access dell'Università di Torino

Oxidative esterification of renewable furfural on gold-based catalysts: Which is the best support?

This is the author's manuscript

Original Citation:

Availability:

This version is available http://hdl.handle.net/2318/141626 since 2016-01-08T15:13:57Z

Published version:

DOI:10.1016/j.jcat.2013.10.005

Terms of use:

Open Access

Anyone can freely access the full text of works made available as "Open Access". Works made available under a Creative Commons license can be used according to the terms and conditions of said license. Use of all other works requires consent of the right holder (author or publisher) if not exempted from copyright protection by the applicable law.

(Article begins on next page)

12 March 2025

UNIVERSITÀ DEGLI STUDI DI TORINO

This Accepted Author Manuscript (AAM) is copyrighted and published by Elsevier. It is posted here by agreement between Elsevier and the University of Turin. Changes resulting from the publishing process - such as editing, corrections, structural formatting, and other quality control mechanisms - may not be reflected in this version of the text. The definitive version of the text was subsequently published in *[Journal of Catalysis, 309, 2014, http://dx.doi.org/10.1016/j.jcat.2013.10.005*].

You may download, copy and otherwise use the AAM for non-commercial purposes provided that your license is limited by the following restrictions:

(1) You may use this AAM for non-commercial purposes only under the terms of the CC-BY-NC-ND license.

(2) The integrity of the work and identification of the author, copyright owner, and publisher must be preserved in any copy.

(3) You must attribute this AAM in the following format: Creative Commons BY-NC-ND license (http://creativecommons.org/licenses/by-nc-nd/4.0/deed.en),[http://ac.els-cdn.com/S0021951713003564/1-s2.0-S0021951713003564-main.pdf?_tid=f24b6752-b360-11e3-a049-00000aab0f26&acdnat=1395671651_615650530d0069ba61206a2460369e18]

Oxidative esterification of renewable furfural on gold based catalysts: which is the best support?

Federica Menegazzo[a], Michela Signoretto*[a], Francesco Pinna[a], Maela Manzoli[b], Valentina Aina[b], Giuseppina Cerrato[b], Flora Boccuzzi[b]

[a] Dept. of Molecular Sciences and Nanosystems
Ca' Foscari University Venice and Consortium INSTM, RU-Venice
Calle Larga S. Marta 2137, 30123 Venice, Italy
Fax: (+) 39(0)41-2348517
*E-mail: miky@unive.it

[b] Dept. of Chemistry & NIS Centre of Excellence
University of Turin
Via P. Giuria 7, 10125 Turin, Italy

Abstract

Gold based catalysts over different supports were investigated in the oxidative esterification of furfural by employing an efficient and sustainable process. The catalytic performances follow the trend: Zirconia-Au > Ceria-Au > > Titania-Au. Zirconia came out to be the best support option to promote activity, selectivity and also stability. The chemical and morphological properties observed for zirconia supported sample seem to fulfil a good compromise between high gold dispersion and the presence of suitable acid-base properties, for good selectivity. Moreover, stability and recycling of the catalysts were also investigated.

Keywords: gold catalyst ; furfural ; oxidation ; biomass ; effect of the support

1. Introduction

With diminishing fossil resources, developing new technologies to utilize versatile and renewable biomass as the alternative feedstock of energy and chemical sources has been attracting more attention than ever. In particular, the upgrading of lignocellulosic biomass wastes into fuels and higher added-value chemicals is one the most researched topics in the forthcoming concept of biorefinery [1].

The sustainability of bio refineries derives from their ability of exploiting every product. Furfural (2-FA), a C5 compound, is industrially manufactured for a long time through hydrolysis of pentose

which comes from agricultural raw materials including corncobs, oat, wheat bran, sawdust, etc. These materials are annually renewable and not competitive with human beings. Thus, exploring the by-products from furfural as the replacements of fossil resources is greatly attractive. In fact, utilization of furfural as the starting material could synthesize a variety of chemicals including more than 1600 commercial products [2].

Actually furfural has many different uses: it is considered an excellent solvent for many organic materials, and it can also be used as a feedstock to make gasoline, diesel, or jet fuel [3]. It is also a precursor to other desired compounds such as furfuryl alcohol (via hydrogenation), furan (via decarbonylation) and tetrahydrofuran (via hydrogenation of furan). Likewise, it can serve as the starting material for the production of 5-hydroxymethylfurfural (by way of hydroxymethylation with formaldehyde). However, additional transformations of furfural are highly desired. The synthesis of alkyl furoates can open very interesting perspectives for the use of xyloses because they find applications as flavour and fragrance component in the fine chemical industry.

Up to now, only a few studies have investigated the heterogeneous catalysis in oxidation of 2-FA [4, 5]. Traditionally, the ester is prepared by oxidizing furfural with potassium permanganate, preferably using acetone as solvent, and reacting the furoic acid so formed with methyl or ethyl alcohol, in the presence of sulphuric acid. The use of these substances have a substantial negative impact on the environment. It has been shown [4] that furfural can be converted to methyl furoate under mild conditions by an oxidative esterification with $NaCH_3O$ and CH_3OH on the Au/TiO_2 reference catalyst purchased from the World Gold Council (WGC) [6]. Very recently we have observed [7] good catalytic performances during esterification of furfural over a gold-supported sulphated zirconia support, especially when compared with the Au/TiO_2 reference catalyst.

Afterwards we have investigated a series of Au/ZrO_2 catalysts calcined at different temperature (from 150°C up to 650°C) in order to modulate the size of the gold nanoparticles, demonstrating that in this reaction, the catalytic activity is strictly connected to the metal dispersion. In particular, the presence of highly dispersed gold clusters ability to activate atomic oxygen is required for good catalytic performances. Moreover, the stability of these new catalysts has been also studied [8]. We demonstrated that the catalytic activity can be completely recovered when the organic residue of the exhausted sample is removed from both gold and zirconia sites [8]. Such results suggested that the support also plays a role in the furfural esterification reaction.

Therefore, we decided to investigate different oxidic supports that are commonly used in catalysis. In particular, we examined plain titania (TiO_2), ceria (CeO_2), and zirconia (ZrO_2). TiO_2 is widely used for a variety of applications because of its high photocatalytic activity, non-toxicity, good availability, low cost, and stability. Its main characteristics strongly depend on its physico-chemical

properties, such as surface area, crystal structure (anatase, rutile, brookite), crystallite size, and surface hydroxyl groups [9]. Ceria is characterized by a high oxygen storage capacity and reducibility [10]: we can take advantage of these properties in furfural esterification reaction, in which atomic oxygen produced on gold species play a fundamental role. Finally, the choice of zirconia as a support is due to its intrinsic chemical and physical characteristics that can be adjusted by choosing different precursors and synthesis conditions [11].

The aim of the present work is to verify the role of the nature of the support in the base free oxidative esterification of furfural catalysed by gold-based systems. In particular, the goal is to investigate the above tested catalysts by employing the main characterisation techniques typically used in surface science approach.

2. Materials and Methods

2.1. Catalyst preparation

$Zr(OH)_4$ was prepared by precipitation from $ZrOCl_2 \cdot 8H_2O$ at constant pH= 8.6 and then aged for 20 hours at 90 °C [12].Then zirconium hydroxide was calcined in air (30 mL/min STP) at 650 °C for 3 hours.

Ceria support was synthesized by precipitation from $(NH_4)_2Ce(NO_3)_6$ by urea at 100 °C in aqueous solution [13, 14]. The solution was mixed and boiled for 6 h at 100 °C, the precipitate was washed twice in boiling deionized water and dried at 110 °C overnight. The material was then calcined in flowing air (50 mL/min) at 650 °C for 3 hours.

Titanium hydroxide was precipitated at pH=8.0 from 0.5 M titanyl sulphate aqueous solution [9]. In particular, 40 g of $TiOSO_4$ xH_2SO_4 yH_2O (Aldrich) were dissolved in 300 mL of distilled water at room temperature under vigorous stirring. The $Ti(OH)_4$ precipitation was obtained by the drop wise addition of 9 M ammonia solution under vigorous stirring. The suspension was magnetically stirred at 60 °C for 20 hours. Then the precipitate was filtered, washed with distilled water in order to remove SO_4^{2-} ions and dried at 110 °C for 18 hours. The absence of sulphates in the material was verified by IEC analysis. Finally the hydroxide was calcined in air flow at 300 °C for 4 hours.

In all cases, gold was added by deposition-precipitation (DP) method at pH=8.6. The oxide supports were suspended in an aqueous solution of $HAuCl_4 \cdot 3H_2O$ for 3 hours and the pH was controlled by the addition of NaOH (0,5 M). After filtration the samples were dried at 35 °C overnight and finally calcined in air for 1 hour at 300 °C. Samples where denoted as Z-Au, C-Au and T-Au.

Oxidative treatments of the exhausted catalysts were carried out with a temperature rate of 2 °C/min from 25 °C to 300 °C in a 5%O_2/He flow (40 mL/min).

2.2. Catalyst characterization method

The sulphate content was determined by ion chromatography (IC). Sulphate concentration was calculated as the average of two independent analyses, each including two chromatographic determinations.

The gold amount for both fresh and exhausted catalysts was determined by atomic absorption spectroscopy (AAS) after microwave disgregation of the samples (100 mg) using a Perkin-Elmer Analyst 100.

Surface areas and pore size distributions were obtained from N_2 adsorption/desorption isotherms at -196 °C (using a Micromeritics ASAP 2000 analyser). Surface area was calculated from the N_2 adsorption isotherm by the BET equation, and pore size distribution was determined by the BJH method [15]. Total pore volume was taken at p/p0 = 0.99.

High resolution transmission microscopy (HRTEM) analysis was performed on all catalysts using a side entry Jeol JEM 3010 (300 kV) microscope equipped with a LaB6 filament and fitted with X-ray EDS analysis by a Link ISIS 200 detector. For analyses, the powdered samples were deposited on a copper grid, coated with a porous carbon film. All digital micrographs were acquired by an Ultrascan 1000 camera and the images were processed by Gatan digital micrograph. A statistically representative number of particles was counted in order to obtain the particle size distribution.

CO pulse chemisorption measurements were performed at -116 °C in a lab-made equipment. Before the analysis, the following pretreatment was applied: the sample (200 mg) was reduced in a H_2 flow (40 mL/min) at 150 °C for 60 min, cooled in H_2 to room temperature, purged in He flow, and finally hydrated at room temperature. The hydration treatment was performed by contacting the sample with a He flow (10 mL/min) saturated with a proper amount of water. The sample was then cooled in He flow to the temperature chosen for CO chemisorption (-116 °C) [16].

FTIR spectra were obtained on a BRUKER IFS28 spectrophotometer (resolution: 2 cm-1, MCT detector). All materials were inspected in the form of self-supporting pellets (about 10 mg cm^{-2}). All samples were activated in a controlled atmosphere at 300°C for ~ 1 hour in a controlled atmosphere (O_2, ~ 60 Torr;) in quartz cells that were connected to a gas vacuum line and equipped with mechanical and turbo molecular pumps (residual pressure $p<10^{-5}$ Torr). BT (IR beam temperature, ~50 °C) CO_2 adsorption (~20 Torr) and desorption (up to 30 min of direct pumping off in vacuo) measurements were carried out in a strictly in situ configuration that allowed background subtraction and spectra rationings.

TPO measurements were carried out in a lab-made equipment: samples (100 mg) were heated with a temperature rate of 10 °C/min from 25 °C to 600 °C in a 5%O_2/He flow (40 mL/min). The effluent gases were analyzed by a TCD detector and by a Genesys 422 quadrupole mass analyzer (QMS).

2.3. Catalytic activity measurements

2-FA oxidative esterification with oxygen and methanol was investigated at 120 °C, without $NaCH_3O$ addition, using a mechanical stirred autoclave fitted with an external jacket [8]. Catalyst (100 mg), 2-FA (Sigma Aldrich, ›99%; 300 μL) and n-octane (Sigma Aldrich, ›99%; 150 μL), used as internal standard, were added to the solvent (150 mL of methanol). The reactor was charged with oxygen (6 bar) and stirred at 1000 rpm. The progress of the reaction was determined after 90 min by gas-chromatographic analysis of the converted mixture (capillary column HP-5, FID detector).

3 Results and Discussion

3.1. Texture, morphology, and structure of the catalysts

N_2 physisorption analyses were carried out in order to determine surface areas and pore size distributions of both supports and catalysts. No significant differences between the N_2 physisorption analyses of the bare supports and those of the corresponding gold based samples have been evidenced. The isotherms for the catalysts are shown in Figure 1, while the corresponding data are reported in Table 1.

The C-Au and T-Au samples exhibited isotherms with hysteresis loops typical of mesoporous materials with unimodal pore size distribution. The adsorption for Z-Au sample shifted towards higher values, indicating the presence of larger pores. Ceria and titania based catalysts exhibited surface area values of 105 m^2/g and 166 m^2/g respectively, while zirconia exhibited the lowest surface area (≈ 40 m^2/g).

CO pulse chemisorption measurements were performed in order to obtain information on the amount of highly uncoordinated Au sites exposed at the surface of the different samples. This way, it is possible to evidence the highly dispersed Au sites escaping from HRTEM detection. We have previously developed a procedure based on the combined use of pulsed CO chemisorption measurements and FTIR spectroscopy of adsorbed CO in well controlled experimental conditions to dose low coordination gold sites exposed at the surface of TiO_2 and CeO_2 oxides [17]. Subsequently, we have proved that this method is suitable also for the quantitative determination of the gold sites on Au/ZrO_2 catalysts [16]. Chemisorption data are reported in Table 1 as molCO/molAu ratio, and they allow us to directly compare all samples, as they refer to the number

of moles of Au in each sample. CO chemisorption also gives a measure of gold dispersion and it can be related to the respective catalytic performances. A high molCO/molAu ratio indicates the presence of clusters that are able to activate molecular oxygen producing atomic O species and thereby rendering the catalyst more active for furfural esterification reaction [8]. The volumetric experiments showed that the molar ratio between adsorbed CO and gold on Z-Au is quite high, indicating the presence of gold clusters. An intermediate value of the ratio was obtained for gold supported on ceria, for which a small amount of Au clusters was present. The sample supported on titania presented the lowest molCO/molAu value, indicating that almost only large Au particles were present on this catalyst.

A careful HRTEM analysis was carried out in order to focus on the gold dispersion on the different supports. The results are resumed in Figure 2 where a HRTEM representative image and the metal particle size distribution for each sample are shown. The measurements revealed the presence of very small roundish Au particles with average size of 2.3±1.1 nm on the Z-Au catalyst with a quite narrow and symmetric particle size distribution, indicating that the gold nanoparticles had homogeneous size. However, we were not able to detect gold particles of even smaller size by means of HRTEM, but we were aware of their presence from CO chemisorption data.

On C-Au, HRTEM measurements evidenced the presence of Au particles with average size of 2.0±1.4 nm. The particle size distribution was quite narrow and symmetric and it was shifted towards smaller sizes. However, chemisorption data revealed a small amount of chemisorbed CO, indicating that on this sample the amount of clusters was smaller than that of the zirconia supported catalysts.

T-Au contained gold nanoparticles with average diameter of 4.2±1.5 nm, meaning that large gold particles only were present on this catalyst. This inference is in good agreement with CO chemisorptions. Moreover, when compared to those of the other samples, the particle size distribution of this sample was very broad ranging between 2 and 11 nm.

3.2. Catalytic performances in the furfural oxidative esterification reaction

The catalysts were tested in the oxidative esterification of furfural to methyl-2-furoate (see Scheme 1). Such reaction was carried out in methanol without the addition of $NaCH_3O$, which would potentially make the esterification process less environmentally friendly and more expensive [5]. A part from 2-MF, the only by-product that was found is the acetal derivate, as reveal by mass spectroscopy.

2-furaldehyde (2-FA)
(reagent)

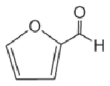

methyl-2-furoate (2-MF)
(product)

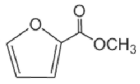

2-furaldehyde-dimethyl-acetal
(by-product)

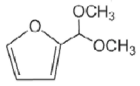

Scheme 1

In Figure 3 the conversions and the 2-MF selectivities after 90 minutes of reaction are reported. Z-Au catalyst showed very good catalytic performances for both conversion (82%) and selectivity (92%). The catalytic performance of this sample was due to the very high dispersion of the gold active phase, as indicated by CO chemisorption data. The Au clusters are able to activate molecular oxygen producing atomic O species that render the catalysts more active for furfural esterification reaction [8]. The C-Au catalyst showed a lower conversion (66%) than Z-Au sample. The molCO/molAu ratio obtained for this catalyst was 0.06, indicating the presence of small gold nanoparticles. Selectivity was much lower if compared to the zirconia catalyst. In fact, this sample presented a remarkable formation of 2-furaldehyde-dimethyl-acetal. The conversion for the T-Au catalyst was very low (20%), according to the presence of big gold particles with size around 4 nm, even if the selectivity was surprisingly good and on a par with the value attained by Z-Au sample (above 90%).

All these results quite clearly indicate that gold dispersion is a crucial factor controlling conversion. However, gold dispersion itself cannot explain the trend observed as for selectivity. Table 1 reports the gold content for each sample, which is in the 1-2 wt% range. Despite a lower Au loading, if compared to the other catalysts, the zirconia supported sample presented the best catalytic results, indicating a vital role played by the support. To accommodate this anomaly, we normalized the catalytic conversion towards a BET specific surface area: see Table 2. It is well known from the literature [18] that despite the much lower SSA exhibited by the zirconia-based catalyst, it always exhibits the best catalytic performance, as activity is strongly influenced by reactivity of the support. In order to shed some light on this aspect, we performed FTIR spectra relative to the adsorption/desorption of CO_2 at BT.

3.3. FTIR spectra of adsorbed CO_2

When present, CO_2 can interact with surface basic sites, like O_2^- anions if present, forming carbonate- and/or bicarbonate-like (hydrogen-carbonate) species [19]. These species are characterised by peculiar IR bands in the 2000-1000 cm^{-1}. Their resistance to outgassing is a clear indication of their stability. Figure 4 provides the main spectroscopic features indicating the interaction between the probe molecule and the different Au-based catalysts. Prior to adsorption, all samples have been thermally activated in order to get rid of most of the contaminants (water, anions, hydro-carbonaceous residues) typically present on the surface of such oxidic systems. In Figure 4 all the spectral patterns are reported as differential spectra obtained by subtracting the contribution of the spectrum relative to the plain activated sample from the spectra of the adsorbed or desorbed probe molecule. Accordingly, all the bands correspond to species which form or resist to adsorption or desorption respectively. The detailed analysis of the various spectral patterns reveals that on T-Au and Z-Au (see the corresponding curves in Figure 4) there is a fair formation of:

carbonate-like species, due to the "side-on" coordination of CO_2 onto pairs of coordinatively unsaturated (cus) $O_2^{- -} M^{n+}$ ions; the spectral components corresponding to the formation of these species are quite complicated by many factors, among which are the natural width of the bands, the presence of band pairs for each kind of carbonate (due to the symmetric and antysimmetric ν of the O-C-O groups), and the large variety of species formed;

bicarbonate-like species (indicated by B and evidenced by the green dotted line), due to the interaction of CO_2 with suitably located free OH groups. B species exhibit, besides the O-C-O stretching modes pair (visible at ~1620 and ~1450 cm^{-1}), a rather narrow peak at ~3610 cm^{-1} (stretching, νOH; not reported for the sake of brevity), and a ~1225 cm^{-1} (bending, σOH) vibration.

Moreover, it can be mentioned that the main carbonate-like species formed mono-dentate species (with spectral components located at ~1590, 1420-1430 and 1310 cm^{-1}) for all systems [20]. However, only in the case of the T-Au sample a peculiar band located at 1380 cm^{-1} was evident: this was due to the $\Sigma\gamma+$ mode of the CO_2 molecule involved in linear coordination with surface cationic sites, i.e. Ti^{4+} ions, present at the surface of the catalyst, thus revealing a residual (somewhat important) Lewis acidity.

As for the C-Au system, carbonate-like species still formed, but had little in common with those formed in the other Au-based systems. This indicates that their structure is typical of the so-called bi-dentate carbonates, which are characterized by the v (O-C-O) modes in the 1680-1790 cm^{-1} spectral range and below ~ 1200 cm^{-1}. These species are structures that are bridging through two

O species of the carbonate molecule and one surface cation, i.e. Me^{n+} species, and are typical of the medium-high dehydration stages of oxides [21]. Moreover, one cannot exclude the formation of hydrogeno-carbonate species for this system; as very weak absorptions are present in their typical positions (see the broken-line arrows reported in Figure 4). In summary, to obtain the best performing catalyst activity, both gold dispersion (for good conversion) and acid/base properties of the support (for good selectivity) must be taken into account. In order to check if a trend can be put into evidence, we took the spectral component located at ~ 1224 cm^{-1} as a "measure" of the intrinsic reactivity of the various supports: the integrated area of this component has been reported in Table 2. It can be observed that the trend is the following: Z-Au >> T-Au >> C-Au. On the basis of all the obtained results, it can be concluded that the presence of suitably located free OH groups, which bring about the formation of hydrogeno-carbonate species, is vital to lead to a good catalytic activity. This is achieved in the case of zirconia-supported catalyst, for which a high gold dispersion is observed as well. In the case of the T-Au sample, which exhibits a quite good amount of Ti^{4+}-OH species that can explain its intrinsic good selectivity, its low conversion value can be justified by the worst Au dispersion. Finally, C-Au system possesses good conversion, due to its good Au dispersion, but exhibits low selectivity due to the poor reactivity of its surface leading to the formation of hydrogeno-carbonate species.

3.4. Investigation on stability and reusability of the catalysts

Catalysts deactivation is a major challenge in catalytic processes. However, tracing the origin of deactivation is often difficult, due to several simultaneously occurring mechanisms contributing to the loss of activity and selectivity. A better understanding of the deactivation processes is essential in order to minimize additional costs and for improving and/or optimizing (i) process conditions, (ii) catalysts design and (iii) for preventing premature catalyst degradation. Combined with the relatively high price of gold, improved stability of the catalyst will add competitiveness to a technology. The study of catalyst deactivation is mainly a characterization oriented problem, as the relevant main mechanisms are sintering, metal leaching and poisoning. Sintering, which is considered to be an irreversible phenomenon, leads to a reduction of the active surface area. Loss of active components by leaching also leads to catalyst deactivation. Either reactants or products generated from the main or side reactions may accumulate at the active surface; carbon containing species may build up on the surface and poison or physically block the active sites.

Very recently we have investigated the stability of gold based catalysts supported on sulphated zirconia in the furfural oxidative esterification [8]. We have ruled out metal leaching and gold sintering problems throughout the reaction time as the cause of deactivation of our catalysts.

As revealed by both TPO and FTIR analyses, the reason for catalysts deactivation is due to their tendency to adsorb organic-like species that accumulate during the reaction. The deactivation is reversible and, after heating in oxygen atmosphere at a proper temperature (450 °C), the catalyst surface is again set free by evolution of carbon dioxide [8]. Such oxidation treatment of the exhausted catalyst allows to almost completely recovering catalytic performances [8].

The TPO profiles of the various catalysts after reaction have been reported in Figure 5. The presence of one broad band that starts at about 150 °C and closes at 500 °C was formed in the curve of Z-Au. The band is due to CO2 evolution, as confirmed by mass spectroscopy that generates from the decomposition of organic species present at the surface of the catalyst. Therefore, the catalyst has been heated in oxygen atmosphere at 450 °C, in order to eliminate the contaminants. After regeneration at 450 °C in oxygen, the catalytic performance of the Z-Au sample is almost completely recovered, as reported in Figure 6.

On the other hand, the TPO profile of the spent T-Au catalyst presents two peaks centred at 250 °C (broad) and 360 °C (very sharp), respectively, suggest that very low conversion data was observed due to the poisoning of the surface large gold particles. When compared with Z-Au sample, both conversion and selectivity of the T-Au sample are very low after the same thermal regeneration in oxygen. However, conversion increases slightly, whilst selectivity drops down. Characterization data have shown that, after the first reaction, the exhausted T-Au sample has only 0.81 wt% of gold, indicating that the catalyst is strongly affected by metal leaching in the reaction medium. In this case the calcination treatment at 300 °C is then likely not sufficient to establish a strong metal/support interaction. We can conclude that the T-Au sample is not recyclable and it is not suitable for this catalytic reaction.

The TPO of the exhausted C-Au sample presents two very weak peaks at 180 °C (very broad) and 350 °C (sharp), indicating the higher reducibility of the ceria support compared to the other systems. After regeneration, the catalytic performances are similar to that of the prepared sample, as shown in Figure 6. This result might be due a partial covering of the surface by contaminants. The C-Au catalyst is therefore recyclable, and presents no gold leaching during the reaction.

4. Conclusion

Gold based catalysts were investigated in the oxidative esterification of furfural by an efficient and sustainable process. The furoate ester can be obtained with optimal yields by a process more environmentally friendly than the actual one.

A comparison among metals, such as Zirconium, Cerium, and Titanium, as a support for Au-based catalysis was performed. Catalytic performances followed the trend of Z-Au > C-Au >> T-Au. Both chemical and morphological properties, such as (i) high dispersion of Au, (ii) specific surface area of the support, and (iii) proper surface sites on the support itself, influence the esterification process. While the surface area of the support influenced the conversion, surface sites affected the selectivity in the process. In this study, zirconium proved to be the ideal support for Au-based oxidation of furfural as it is active, selective, recyclable, and applicable in a biomass based renewables producing industry.

Acknowledgments

We thank Mrs. Tania Fantinel for technical assistance. Financial support to this work by MIUR (Cofin 2008) is gratefully acknowledged.

References

1 I. Agirrezabal-Telleria, J. Requies, M.B. Güemez, P.L. Arias, Appl. Catal. B 115– 116 (2012) 169– 178.

2 H. Guo, G. Yin, J. Phys. Chem. C 115 (2011) 17516–17522.

3 R. Weingarten, J. Cho, C. Conner, G. W. Huber, Green Chem. 12 (2010) 1423–1429.

4 E. Taaring, I. S. Nielsen, K. Egeblad, R. Madsen, C.H. Christensen, ChemSusChem 1 (2008) 75-78.

5 O. Casanova, S. Iborra, A. Corma, J.Catal. 265 (2009) 109-116.

6 Sample number 17C, supplied by World Gold Council, http://www.gold.org.

7 F. Pinna, A. Olivo, V. Trevisan, F. Menegazzo, M. Signoretto, M. Manzoli, F. Boccuzzi, Catal. Today 203 (2013) 196-201.

8 M. Signoretto, F. Menegazzo, L. Contessotto, F. Pinna, M. Manzoli, F. Boccuzzi, Appl. Catal. B 129 (2013) 287-293.

9 V. Trevisan, M. Signoretto, F. Pinna, G. Cruciani, G. Cerrato, Chemistry Today 30 (2012) 25-28.

10 A. Trovarelli, Catal. Rev. –Sci. Eng. 38 (1996) 439-520.

11 X. Song, A. Sayari, Catal. Rev.–Sci. Eng. 38 (1996) 329-412.

12 M. Manzoli, F. Boccuzzi, V. Trevisan, F. Menegazzo, M. Signoretto, F. Pinna, Appl. Catal. B. 96 (2010) 28-33.

13 L. Kundakovic, M. Flytzani-Stephanopoulos, J. Catal. 179 (1998) 203-221.

14 F. Menegazzo, P. Burti, M. Signoretto, M. Manzoli, S. Vankova, F. Boccuzzi, F. Pinna, G. Strukul, J. Catal. 257 (2008) 369-381.

15 S.J. Gregg, K.S.W. Sing, Adsorption, Surface Area and Porosity – 2nd ed., Academic Press, 1982, p. 111.

16 F. Menegazzo, F. Pinna, M. Signoretto, V. Trevisan, F. Boccuzzi, A. Chiorino, M. Manzoli, Appl. Catal. A. 356 (2009) 31-35.

17 F. Menegazzo, M. Manzoli, A. Chiorino, F. Boccuzzi, T. Tabakova, M. Signoretto, F. Pinna, N. Pernicone, J. Catal. 237 (2006) 431-434.

18 F. Moreau, G. C. Bond, Catal. Today 122 (2007) 215-221.

19 G. Busca, V. Lorenzelli, Mater. Chem. 7(1982) 89-126.

20 V. Bolis, G. Magnacca, G. Cerrato, C. Morterra, Top. Catal. 19 (2002) 259-269.

21 C. Morterra, G. Emanuel, G. Cerrato, G. Magnacca, J. Chem. Soc. Faraday Trans. 88 (1992) 339-348.

Table 1. Physico-chemical properties of the samples and catalytic performances.

	Au/ZrO_2 Z-Au	Au/CeO_2 C-Au	Au/TiO_2 T-Au
Surface area (m^2/g)	39	105	166
Pore diameter (nm)	21	5	4
Pore volume (cm^3/g)	0.26	0.16	0.21
Au loading (%)	1.0	2.2	1.2
Chemisorption mol_{CO}/mol_{Au})	0.24	0.06	0.004

Table 2. Comparison between the "normalized" catalytic conversion and the integrated area of the 1224 cm^{-1} spectral component

Sample	Conversion/SSA *	Integrated area of the 1224 cm^{-1} spectral component
Z-Au	82/39 = 2.1	2.89
C-Au	66/105 = 0.62	0.15
T-Au	20/166 = 0.12	0.68

***** obtained normalizing the catalytic conversion towards the BET specific surface area

Figure 1: N_2 physisorption isotherms of the catalysts and (insert) their BHJ pore size distributions.

Figure 2: HRTEM images of calcined catalysts and gold particle size distribution. The images were taken at an original magnification of 300000X.

Figure 3: Catalytic performances after 90 minutes of reaction.

Figure 4. Differential spectra relative to CO_2 adsorption/desorption at BT onto the different Au-supported catalysts. Black curves refer to the adsorption of the probe molecule, whereas red curves refer to the desorption (i.e., pumping off) in vacuo for 30 min.

Figure 5: TPO of the exhausted catalyst after 90 minutes of reaction

Figure 6: Catalytic performances in the reuse tests

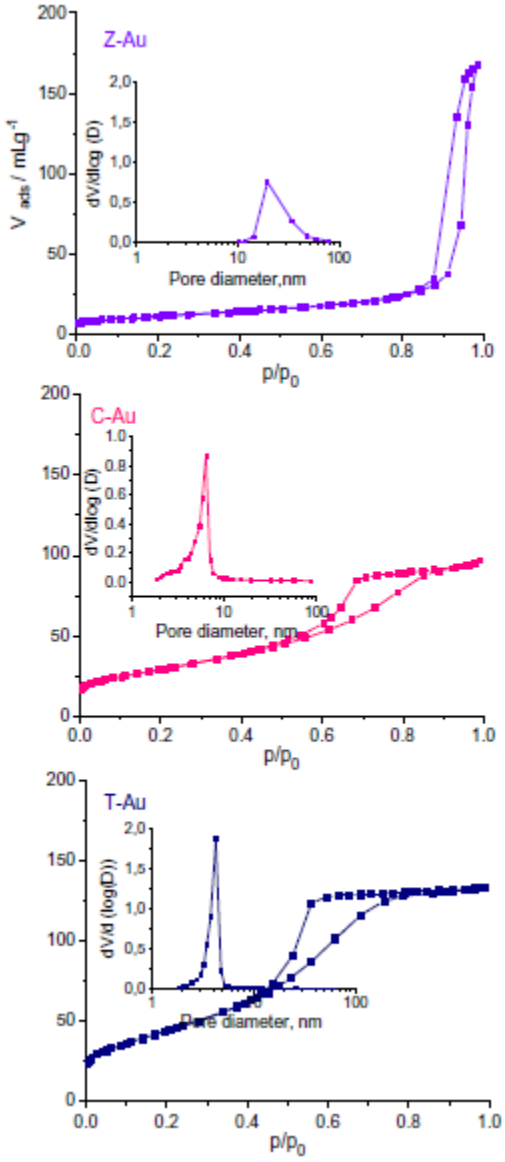
Z-Au
V ads / mLg-1
dV/dlog (D)
Pore diameter,nm
p/p0
C-Au
dV/dlog (D)
Pore diameter, nm
p/p0
T-Au
dV/d (logD))
Pore diameter, nm
p/p0

Fig.1

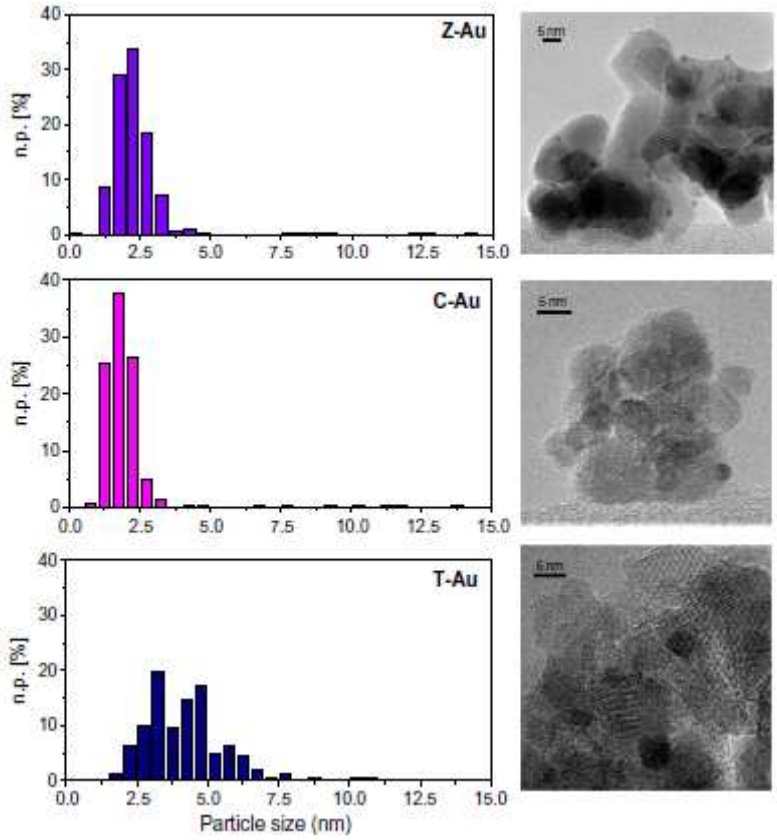

Fig. 2

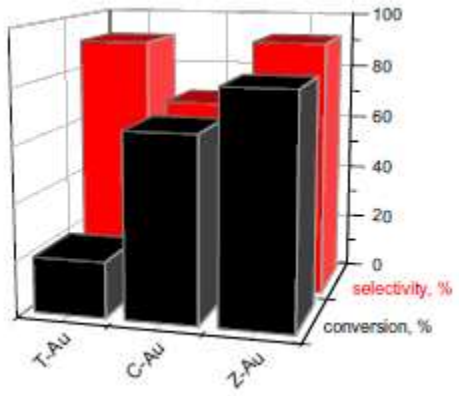

Fig. 3

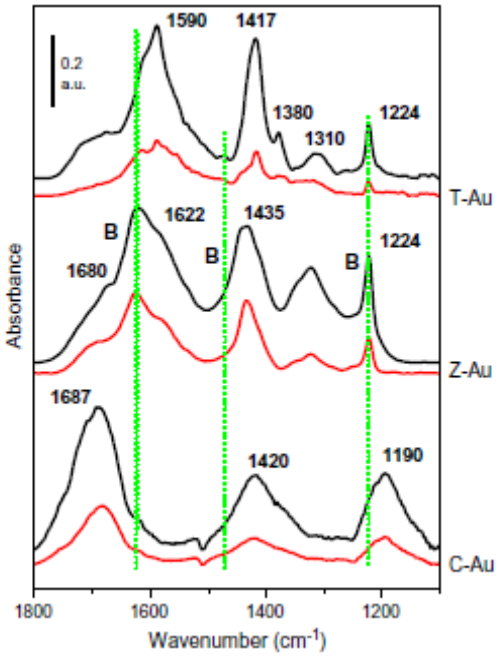
0.2
a.u.
1590
1417
1380
1310
1224
T-Au
B
1680
1622
B
1435
B
1224
Z-Au
1687
1420
1190
C-Au
Absorbance
1800
1600
1400
1200
Wavenumber (cm-1)

Fig. 4

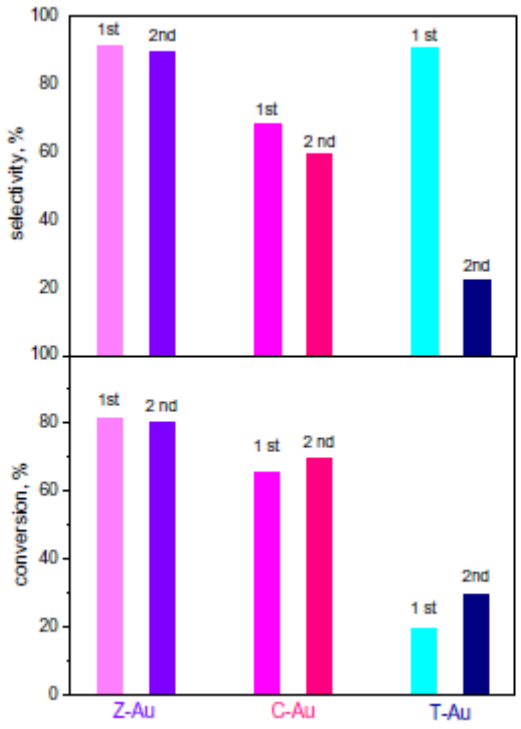
selectivity, %
conversion, %
1st
2nd
1st
2 nd
1 st
2nd
1st
2 nd
1 st
2 nd
1 st
2nd
Z-Au
C-Au
T-Au

Fig. 5

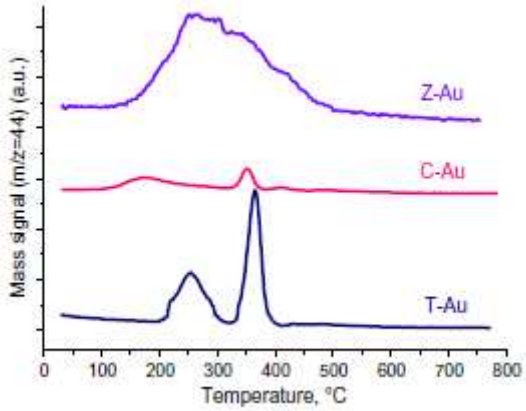
Mass signal (m/z=44) (a.u.)
Z-Au
C-Au
T-Au
0
100
200
300
400
500
600
700
800
Temperature, °C

Fig. 6

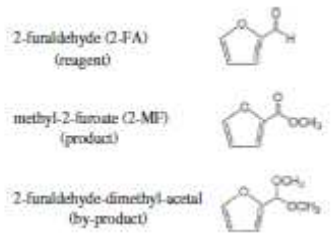
2-furaldehyde (2-FA)
(reagent)
methyl-2-furoate (2-MF)
(product)
2-furaldehyde-dimethyl-acetal
(by-product)

Scheme 1